LBL-37830
UC-408
Preprint

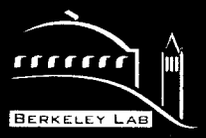

ERNEST ORLANDO LAWRENCE
BERKELEY NATIONAL LABORATORY

Consequences of Using a Simplified Kinetic Model for Dynamic PET Data

P.G. Coxson, R.H. Huesman, and L. Borland
Life Sciences Division

October 1995
Submitted to *Journal of Nuclear Medicine*

LBL–37830

Consequences of Using a Simplified Kinetic Model for Dynamic PET Data

Pamela G. Coxson[a] Ph.D., Ronald H. Huesman[a] Ph.D., Lisa Borland[b] Ph.D.

[a]Center for Functional Imaging, Lawrence Berkeley National Laboratory, University of California, Berkeley, CA 94720
[b]Department of Physics, University of California, Berkeley, CA 94720

This work was supported in part by the National Heart, Lung and Blood Institute of the U.S. Department of Health and Human Services under Grants No. HL47675, HL25840 and HL07367, and in part by the Director, Office of Energy Research, Office of Health and Environmental Research, Medical Applications and Biophysical Research Division of the U.S. Department of Energy under Contract No. DE-AC03-76SF00098.

Running Title: Dynamic PET Kinetic Models

Keywords: positron emission tomography, physiological models, model comparisons, rubidium-82, myocardial blood flow

ABSTRACT

A physiological model of ^{82}Rb kinetics in the myocardium was compared with two reduced-order models with regard to their ability to assess physiological parameters from dynamic positron emission tomography (PET) data. **Methods.** A three-compartment model of ^{82}Rb in the myocardium was used to simulate kinetic PET region of interest data. Simulations were generated for eight different blood flow rates reflecting the physiological range of interest. Two reduced-order models commonly used with myocardial PET studies were fit to the simulated data, and parameters of the reduced-order models were compared with the physiological parameters. Then all three models were fit to the simulated data with noise added. Monte Carlo simulations were used to evaluate and compare the diagnostic utility of the reduced-order models. A description length criterion was used to assess goodness-of-fit for each model. Finally, fits to simulated data were compared with fits to actual dynamic PET data. **Results.** Fits of the reduced-order models to the three-compartment model noise-free simulated data produced model misspecification artifacts such as flow parameter bias and systematic variation with flow in estimates of non-flow parameters. Monte Carlo simulations showed some of the parameter estimates for the two-compartment model to be highly variable at PET noise levels. Fits to actual PET data showed similar variability. One-compartment model estimates of the flow parameter at high and low flow were separated by several standard deviations for both the simulated and the real data. With the two-compartment model, the separation was about one standard deviation, making it difficult to differentiate a high and a low flow in a single experiment. Fixing non-flow parameters reduced flow parameter variability in the two-compartment model, and did not significantly affect variability in the one-compartment model. Goodness-of-fit indicated that at realistic noise levels both reduced-order models fit the simulated data at least as well as the three-compartment model that generated the data. **Conclusions.** The one-compartment reduced-order model of ^{82}Rb dynamic PET data can be used effectively to compare myocardial blood flow rates at rest and stress levels. The two-compartment model can differentiate flow only if *a priori* values are used for non-flow parameters.

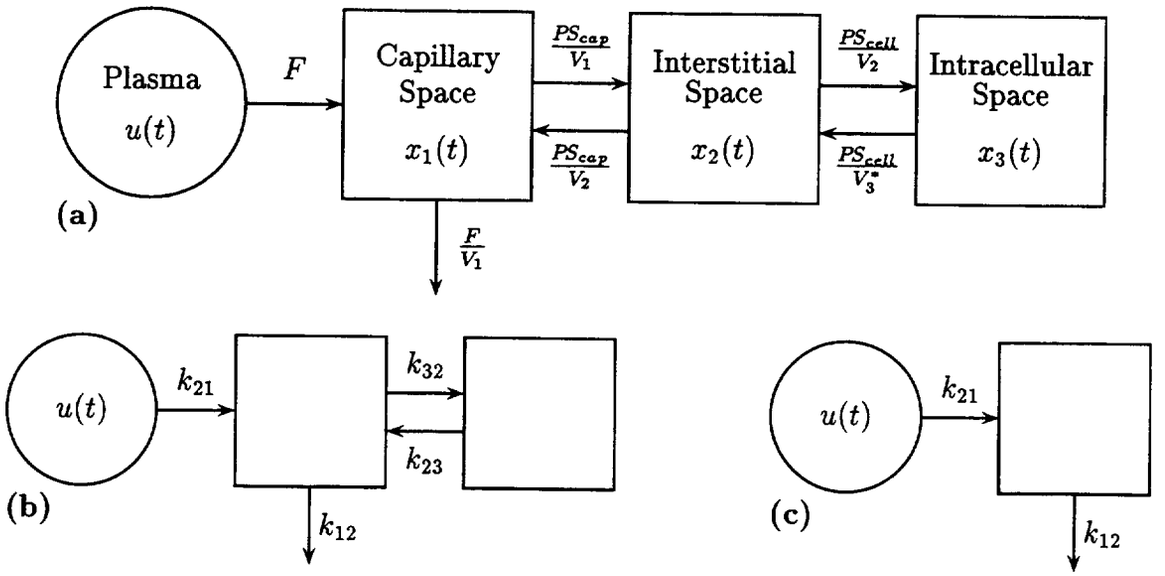

Figure 1: Compartmental Models of ^{82}Rb in the Myocardium. (a) The three compartment physiological model has parameters PS_{cap} and PS_{cell}, permeability surface products for the capillary and cell walls, fractional volumes (V_i) of the spatial compartments, and specific volume blood flow (F). (b) In the two-compartment model, plasma and interstitial compartments are lumped on the assumption that they equilibrate rapidly. (c) The one-compartment model has uptake and washout parameters only.

Introduction

Compartmental models represented by systems of linear differential equations are used to describe the time evolution of kinetic region of interest data from a positron emission tomograph [1]. A three-compartment model of the disposition of ^{82}Rb in the myocardium is shown in Figure 1a, and the corresponding system of differential equations is:

$$\dot{x}_1(t) = -\left(\frac{F}{V_1} + \frac{PS_{cap}}{V_1}\right) x_1(t) + \frac{PS_{cap}}{V_2} x_2(t) + Fu(t) , \quad (1)$$

$$\dot{x}_2(t) = \frac{PS_{cap}}{V_1} x_1(t) - \left(\frac{PS_{cap}}{V_2} + \frac{PS_{cell}}{V_2}\right) x_2(t) + \frac{PS_{cell}}{V_3^*} x_3(t) , \quad (2)$$

$$\dot{x}_3(t) = \frac{PS_{cell}}{V_2} x_2(t) - \frac{PS_{cell}}{V_3^*} x_3(t) , \quad (3)$$

where $\dot{x}_i(t)$ denotes the time derivative of $x_i(t)$, which is activity in compartment i per volume of tissue.

The compartments are identified with physiological spaces — capillary, interstitial space, and intracellular space. The input function $u(t)$ consists of blood pool concentration of ^{82}Rb

(activity per volume of blood). The transfer rates between compartments are expressed in terms of specific volume blood flow (F), permeability surface products (PS) for two physiological barriers, fractional volumes (V_i) of the interstitial and capillary spaces, and the apparent volume of distribution factor (V_3^*) of ^{82}Rb in the intracellular space. Thus, we refer to this model as a physiological compartmental model. More complex models incorporating features such as heterogeneous flow rates, variable capillary length, and axial diffusion have been used to fit multiple tracer dilution data [2, 3, 4]. However, we will be making comparisons with smaller models and will refer to this three-compartment model as *the* physiological model and to its parameters as *the* physiological parameters.

PET data consist of estimated total emissions from a region of interest. Regions have linear dimensions on the order of millimeters, which are too large to provide separate data for capillary, interstitial, and intracellular compartments. Emission counts estimated from tomographic line integrals are affected by numerous sources of error reflecting both physical limitations [5, 6, 7, 8] and methodological factors [9, 10, 11]. Because of the coarseness of the measurements and the cumulative effect of errors in the measurements, it is not feasible to estimate all of the parameters of Figure 1a from the PET data alone.

For this reason, PET kinetic analysis has typically been carried out with lower order compartmental models. The two- and one-compartment models shown in Figure 1b and 1c are among those which have been employed [12, 13, 14]. The parameter of interest in most PET kinetic studies of the myocardium is specific volume flow (per min) and models are judged on their ability to distinguish between rest flow rates around 1 per min and stress flow rates of 3 or 4 per min.

For all models considered here, the PET measured data $y(t)$ are simulated as a fraction (f_v) of the plasma concentration plus the sum of all compartments $\{x_i\}$:

$$y(t) = f_v\, u(t) + \sum_{i=1}^{n} x_i(t)\ , \tag{4}$$

where n is the number of compartments. Individual measurements y_i represent mean activity over the scanning interval,

$$y_i = \frac{1}{(t_i - t_{i-1})} \int_{t_{i-1}}^{t_i} y(t)dt. \tag{5}$$

Two models are mathematically equivalent if they produce the same measurement values $y(t)$ for the same input function $u(t)$. The two-compartment model would be equivalent to the physiological model if PS_{cap} were infinite. In that case, compartments 1 and 2 of the physiological model could be lumped into a single compartment corresponding to the first compartment of the two-compartment model and the parameters of the reduced model would be as follows:

$$k_{21} = F\ , \tag{6}$$

$$k_{12} = \frac{F}{V_1 + V_2}\ , \tag{7}$$

$$k_{32} = \frac{PS_{cell}}{V_1 + V_2}, \tag{8}$$

$$k_{23} = \frac{PS_{cell}}{V_3^*}. \tag{9}$$

All parameters k_{ij} are in units of inverse minutes.

Since PS_{cap} and PS_{cell} are not infinite, both the two-compartment and the one-compartment models are distinct from the physiological model and estimates of the physiological parameters based on these models will be biased. In the current study we use simulations to examine the effect of fitting the parameters of the one- and two-compartment models to data generated by the physiological model.

Methods

Noise-Free Simulations

Eight simulated PET data sets were created by calculating $y(t)$ for the physiological model with F (flow) set to 0.5, 1.0, 1.5, 2.0, 2.5, 3.0, 3.5, and 4.0 per min, covering the range of physiologic interest. Other model parameters were kept fixed at the following values:

$$PS_{cap} = 5 \text{ min}^{-1} \qquad V_1 = 0.05 \qquad f_v = 0.1$$
$$PS_{cell} = 1 \text{ min}^{-1} \qquad V_2 = 0.25$$
$$V_3^* = 5.0$$

Values for these physiological parameters do not appear in the literature in any one place. Volumes of the capillary, interstitial, and intracellular space for rabbit heart are given as 0.07 ml/g, 0.20 ml/g, and 0.60 ml/g in [15], based in part on detailed measurements in [16]. The proportion of myocardial wall comprised of larger blood vessels is given as 0.08 ml/g, which would be part of the vascular fraction in this model. Fractional interstitial fluid volume in the left ventricle of a dog is estimated to be 0.28 in [17]. PS_{cap} is assumed to be much greater than PS_{cell}. In setting values for these permeability parameters we also took into account findings in [18] and [17]. PS_{cap} was selected to be large, perhaps out of the physiological range, in order to give the benefit of the doubt to the hypothesis of instantaneous exchange between capillary and interstitial fluid. V_3^* was chosen to be consistent with experimental data collected in our group.

An actual ^{82}Rb left ventricular blood pool region of interest data set was used for the input function $u(t)$. The input function and simulated measurement values y_i are shown in Figure 2 for the two extreme rates of flow ($F = 0.5$ per min and $F = 4.0$ per min). All simulations and fits were carried out with an in-house fitting program, using closed-form solutions to the linear differential equations [19]. A weighted least-squares criterion was used to determine a best fit, with the weight on each measurement y_i equal to the reciprocal of y_i^2. (These weights were needed to avoid bias relative to the noisy fits, due solely to the

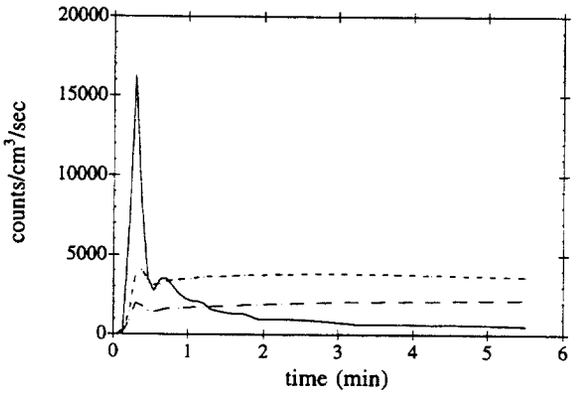

Figure 2: Physiological Model Simulated Data. The blood input function taken from an actual ^{82}Rb PET study is shown (solid line) along with simulated myocardial region of interest data for two flow rates. The long dashed line denotes simulated data for flow equal to 0.5 per min, and the short dashed line denotes simulated data for flow equal to 4.0 per min.

weighting choice for the noisy simulations.) The two reduced-order models were fit to the simulated data from the physiological model.

Monte Carlo Simulations

To test the robustness of the parameter estimates, Monte Carlo simulations were carried out with relative error of zero mean and 1%, 5%, 10% or 20% standard deviation added to the measurement values y_i for the physiological model. The assumption of constant percent measurement noise is reasonably close to our experience with PET data. In dynamic PET data sets, the percent error increases somewhat with time due to isotope decay, but then drops with an increase in scanning time. Since scanning intervals are increased in part to compensate for isotope decay, the effect is to keep the noise level steady. The two reduced-order models were fit to 1000 noisy simulations at each of the eight flow rates for each noise level. Weights for the weighted least squares fit were equal to the inverse variance of y_i.

PET Studies

The three models studied here were also fit to existing ^{82}Rb PET data sets and the results compared to the simulation fits. Data were selected from a data base of human volunteer and animal subject rest-stress studies conducted at the Center for Functional Imaging, Lawrence Berkeley National Laboratory. Human subjects were imaged with a Siemens/CTI ECAT EXACT HR tomograph and were analyzed in sixteen three-dimensional volumes of interest defined as described in [20]. Dog study data were collected with the 600 Crystal Donner

Positron Tomograph under a protocol as described in [14]. Model parameters were estimated in fifteen 8 mm diameter regions of interest in a single slice image through the left ventricle. One human subject rest-stress pair of data sets and one dog study pair are used to draw comparisons with the simulated data results. Data from one region imaged at rest (low flow) and stress (high flow) are plotted in Figure 3 for both of the representative studies.

These dynamic PET data sets differ from the simulated data in a number of ways. The blood input function is the same for all regions of interest from a single dynamic data set, but each separate data set is generated from a separate injection of ^{82}Rb. The stress state input function differs from the rest state input function because of the variability inherent in the injection procedure and also because the different physiological state affects the blood levels so that even two identical injections would produce different blood time activity curves. The blood activity data, collected from the left ventricular blood pool, are noisy. Region of interest data have error percentages which are non-uniform across time and can be different for rest and stress studies in the same subject. The dog study rest state data set (Figure 3) has 12% to 24% error and the stress data set 8% to 17% error at most time points. A similar difference holds for the human study, with rest state percentage errors somewhat greater than stress state errors. Perhaps most important, the underlying dynamic which generated the PET data is not known perfectly and is surely more complex than the three-compartment model used to generate the simulated data.

Goodness-of-Fit Model Comparisons

The weighted least squares criterion used to determine the best fit of a particular model is not useful for comparisons between models because it tends to decrease with increasing model complexity. Model comparisons have to take complexity into account and there are several ways to do this. We compared fitted curves based on the physiological model and the two reduced-order models using the description length criterion [21]:

$$DL = m \log 2\pi + 2 \log \prod_{i=1}^{m} \sigma_i + \sum_{i=1}^{m} \frac{(y_i - \hat{y}_i)^2}{\sigma_i^2} + \frac{p}{2} \log m \ . \tag{10}$$

The description length (DL) of a fitted curve consists of twice the negative log likelihood function plus a term which adds a penalty for the number of fitted parameters (p) and number of data points (m). σ_i^2 denotes the variance of y_i. $\hat{y}_i$ denotes the best weighted least squares fit, obtained previously. A smaller value for DL indicates a better fit. Some readers will be more familiar with the Akaike information criterion (AIC) which differs only in the form of the penalty term. AIC and DL give essentially the same results for the models examined here.

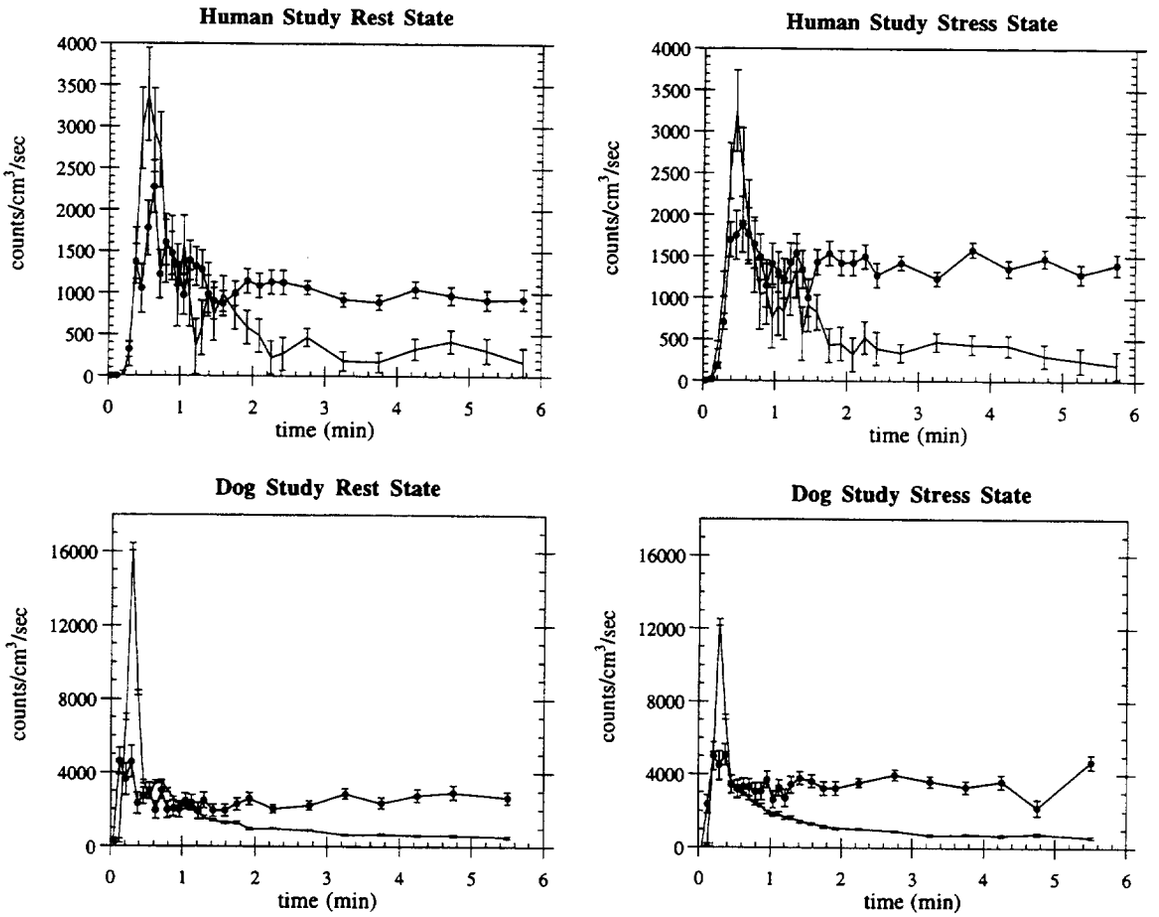

Figure 3: Dynamic PET Data Sets at Rest (low flow) and Stress (high flow). The upper two plots display data from a human subject study and the lower plots contain a similar pair of data sets from a dog study. In each plot, the blood input function $u(t)$ is shown as a solid line with error bars along with the tissue time activity curve for a single myocardial region of interest (solid line with filled circles and error bars) imaged at one of the two physiological states.

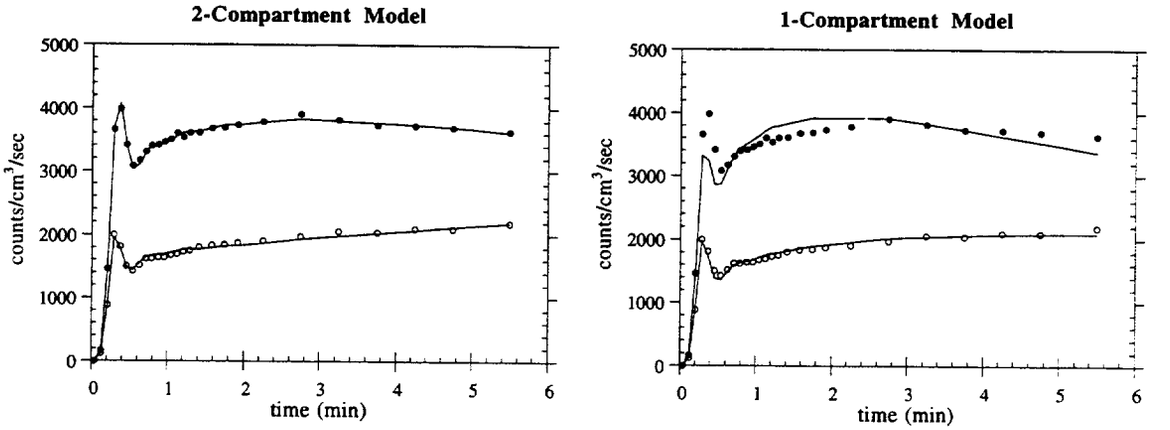

Figure 4: Reduced-Order Model Fits. The best weighted least squares fit (solid line) of the reduced-order model to the physiological model is plotted for low flow ($F = 0.5$ per min, open circles) and high flow ($F = 4.0$ per min, filled circles) data.

Results

No-Noise Fits

Figure 4 shows the best fit of the two reduced-order models to the simulated data from Figure 2 for high and low flow, using the weighted least squares criterion described earlier. The two-compartment model gives a very good fit to both high and low flow data. The one-compartment model is visibly different in shape, especially apparent in the high flow fit.

Parameter values for fits at all eight rates of flow are displayed in Table 1. The two-

Table 1: Noise-Free Simulation Parameter Fits

	2-Compartment					1-Compartment		
F	k_{21}	k_{12}	k_{32}	k_{23}	f_v	k_{21}	k_{12}	f_v
0.5	0.503	2.253	3.730	0.171	0.099	0.346	0.092	0.109
1.0	0.935	3.484	3.286	0.175	0.098	0.529	0.137	0.119
1.5	1.319	5.084	3.491	0.184	0.100	0.630	0.161	0.130
2.0	1.708	6.355	3.345	0.179	0.097	0.701	0.175	0.137
2.5	2.072	7.738	3.360	0.178	0.096	0.748	0.183	0.144
3.0	2.401	9.232	3.493	0.182	0.098	0.779	0.189	0.152
3.5	2.656	10.156	3.489	0.181	0.097	0.802	0.192	0.157
4.0	3.020	11.578	3.462	0.181	0.095	0.820	0.197	0.162

compartment k_{21} parameter underestimated flow, with the greatest disparity at high flow. If one were to assume that PS_{cap} was infinite, the two-compartment model parameters would give estimates of $V_1 + V_2$, PS_{cell}, and V_3^* that are within 15% of the corresponding values in the physiological model:

	Physiological Model	2-Compartment Estimates
$V_1 + V_2$	0.3	0.26 ± 0.01
PS_{cell}	1	0.89 ± 0.03
V_3^*	5	4.99 ± 0.06

The one-compartment k_{21} parameter increased modestly with increasing flow, as did the other two parameters, k_{12} and f_v.

Monte Carlo Simulations

Statistics for the 1000 sets of fitted parameters resulting from the Monte Carlo simulations are summarized for the case of 20% standard deviation in Table 2. Quartiles (25th percentile, median, and 75th percentile) rather than mean and standard deviation are displayed because the distributions of some of the parameter estimates are non-gaussian with tail values that distort the mean. Comparing this table with the noise free results in Table 1 it is clear that the parameter estimates in the noisy case have significant bias and variation.

Although all of the physiological parameters are of interest, we will focus our attention on the flow parameter with the clinical objective of differentiating flow and detecting a three-fold increase in flow. In both reduced-order models, the uptake parameter k_{21} is used as the indicator of flow. In Figure 5, the sample mean and standard deviations for the k_{21} estimates are plotted as a function of flow for both the 10% and 20% noise simulations.

It should be noted here that dynamic PET data with 10% noise would be considered to be very good, and 20% noise is not uncommon. Overlapping distributions of k_{21} values at high flow suggest that neither model would be able to differentiate between different large flow rates such as $F = 3$ per min and $F = 4$ per min, even at the lower noise level. The one-compartment model k_{21} is relatively insensitive at high flow, while the two-compartment model k_{21} estimate is sensitive enough but too variable. The k_{21} estimate of the highest flow ($F = 4$ per min) is separated from that of the lowest flow ($F = 0.5$ per min) by more than one standard deviation in the two-compartment model and by several standard deviations in the one-compartment model, at the 20% noise level.

To visualize the separability of a conservative flow differential, we have plotted the first 20 of 1000 realizations of k_{21} for a low ($F = 1$ per min) and an elevated ($F = 3$ per min) flow for each reduced-order model for the case of 20% noise (Figure 6).

Variability of the two-compartment model k_{21} estimates could be reduced if reasonable estimates of some of the other parameters were available so that those parameters did not have to be estimated. Two plots are included in Figure 6 to illustrate this in the best possible case

Table 2: Noisy Simulation Parameter Fits
1000 Monte Carlo Simulations with 20% Noise

	2-Compartment (lower quartile median upper quartile)					1-Compartment (lower quartile median upper quartile)		
F	k_{21}	k_{12}	k_{32}	k_{23}	f_v	k_{21}	k_{12}	f_v
0.5	0.41	0.45	0.68	-0.09	0.09	0.33	0.06	0.10
	0.50	1.53	2.30	0.06	0.10	0.35	0.09	0.11
	0.65	4.69	5.66	0.19	0.11	0.37	0.12	0.12
1.0	0.72	1.24	1.27	0.01	0.09	0.50	0.10	0.11
	0.91	3.13	2.70	0.11	0.10	0.52	0.13	0.12
	1.15	6.36	5.03	0.21	0.11	0.55	0.16	0.13
1.5	1.05	2.17	1.46	0.06	0.08	0.60	0.13	0.12
	1.36	4.69	2.80	0.14	0.10	0.63	0.16	0.13
	1.71	8.68	5.00	0.23	0.11	0.67	0.20	0.14
2.0	1.35	3.25	1.77	0.08	0.08	0.66	0.14	0.13
	1.71	5.91	2.84	0.15	0.10	0.70	0.18	0.14
	2.09	10.07	4.63	0.22	0.12	0.74	0.21	0.15
2.5	1.66	4.53	1.91	0.10	0.08	0.71	0.15	0.13
	2.11	7.38	3.05	0.16	0.10	0.75	0.19	0.14
	2.54	11.84	4.60	0.23	0.12	0.79	0.22	0.16
3.0	1.89	5.29	2.12	0.09	0.08	0.73	0.15	0.14
	2.39	8.60	3.02	0.16	0.10	0.78	0.19	0.15
	2.91	12.91	4.53	0.22	0.12	0.82	0.22	0.17
3.5	2.17	6.51	2.26	0.11	0.08	0.76	0.15	0.14
	2.74	10.22	3.19	0.16	0.10	0.80	0.19	0.16
	3.36	15.68	4.66	0.22	0.12	0.85	0.23	0.17
4.0	2.44	7.21	2.28	0.11	0.08	0.78	0.16	0.15
	3.01	10.78	3.14	0.17	0.10	0.82	0.20	0.16
	3.61	16.95	4.84	0.22	0.12	0.87	0.23	0.18

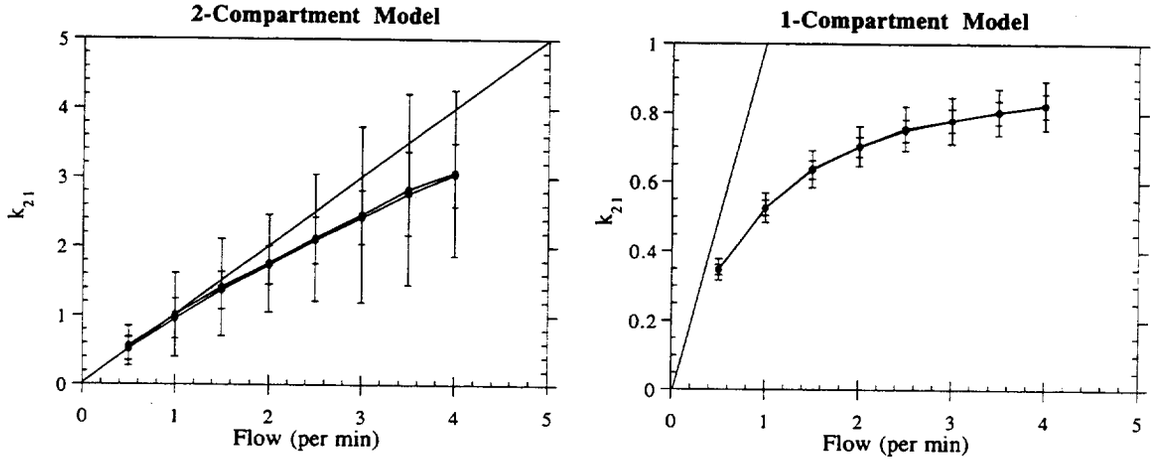

Figure 5: Plots of k_{21} estimates for 10% and 20% noise simulations. Mean values of the k_{21} estimates from Monte Carlo simulations are plotted with error bars representing the sample standard deviations. Estimates for the 20% noise case are shown with open circles and have the larger error bars.

where values are known for all model parameters except flow. For the three-compartment model, parameters were set to their known values used to generate the simulations. The estimates of k_{21} shown for the two-compartment model were obtained with parameters k_{23}, k_{32}, and f_v set to 0.15, 3.0, and 0.1, respectively, and k_{12} constrained to be $k_{21}/0.3$. There are various alternative strategies for fixing parameters of the two-compartment model and the result is qualitatively the same for all the ones we tried (true values assuming infinite PS_{cap}; mean values observed in fits; values chosen to "tune" the model to known flow values, etc.). Variability of the one-compartment model k_{21} estimates is not significantly improved by fixing or constraining other parameters.

PET Studies

Data from dog and human PET studies were fit with the two reduced-order models studied here, and the resulting parameters are shown in Table 3. The values in this table can be compared with the simulated data parameter estimates in Table 2. The earlier table is based on a sample size of 1000 simulations versus the 15 or 16 regions of interest available from the PET study, so we would expect the parameter medians and the variability (represented here by the inter-quartile range) to be quite variable from one study to the next, even in the ideal case where the data satisfied all of the modeling assumptions.

Several similarities and differences are immediately apparent from the tables. The k_{21} estimate increased significantly with flow in the simulations and in the PET studies, with both models. All three parameters in the one-compartment model increased with flow for the PET

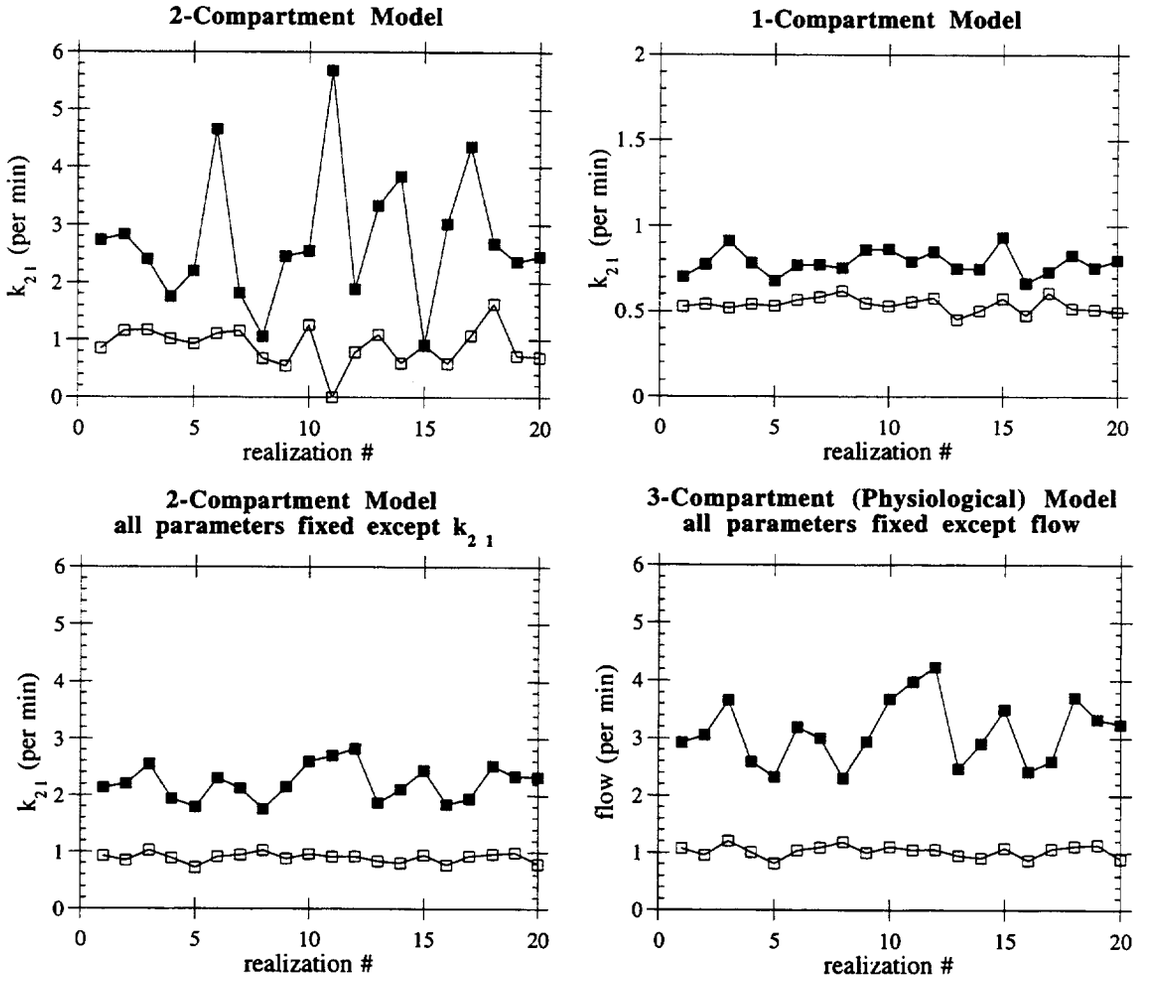

Figure 6: Twenty realizations of k_{21} at $F = 1$ per min and $F = 3$ per min. The first 20 of 1000 k_{21} estimates based on Monte Carlo simulations of the physiological model with 20% noise are displayed for a low and a high flow. The upper plots show values based on fits of all parameters to the two- and one-compartment models (note that the y-axis scales are different for the sake of readability and comparison of qualitative features). Lower plots show the estimates obtained for the two- and three-compartment models if all parameters except k_{21} (or flow) are fixed or constrained.

Table 3: Parameter Fits to Dynamic PET Data

	2-Compartment (lower quartile median upper quartile)					1-Compartment (lower quartile median upper quartile)		
Dog Study (n = 15 regions)	k_{21}	k_{12}	k_{32}	k_{23}	f_v	k_{21}	k_{12}	f_v
Rest	0.40	0.17	0.32	-0.11	0.16	0.36	0.05	0.17
	0.50	0.38	1.81	0.02	0.25	0.39	0.08	0.25
	0.68	2.13	4.95	0.11	0.26	0.44	0.11	0.31
Stress	0.66	0.15	0.09	-0.22	0.16	0.63	0.10	0.25
	0.82	0.23	0.37	0.04	0.25	0.69	0.11	0.31
	5.24	29.90	2.72	0.13	0.31	0.73	0.14	0.35
Human Study (n = 16 regions)	k_{21}	k_{12}	k_{32}	k_{23}	f_v	k_{21}	k_{12}	f_v
Rest	0.31	0.28	1.55	0.10	0.34	0.31	0.04	0.39
	0.35	0.44	50.99	5.70	0.42	0.33	0.07	0.43
	0.52	1.58	97.05	18.60	0.54	0.36	0.10	0.54
Stress	1.13	2.18	1.41	0.17	0.23	0.53	0.17	0.39
	1.76	4.32	1.55	0.21	0.32	0.58	0.18	0.48
	2.91	7.60	2.33	0.32	0.37	0.63	0.20	0.55

studies, as predicted by the simulations. For both the simulations and the PET data, the most variable parameter values are the k_{12} and k_{32} estimates for the two-compartment model. As expected, the variation is greater in the PET study tables. The other two-compartment model parameters and all one-compartment model parameters have significantly smaller inter-quartile ranges in the simulation table and also, with a couple of exceptions, in the PET data tables. The vascular fraction estimates are much greater in the PET studies than the 0.1 value used in the simulations.

If parameters other than k_{21} are fixed or constrained, then k_{21} variability is reduced. For our PET study examples, the fixed values were chosen to be the same as for the fixed parameter fits to the Monte Carlo simulations described in the previous section, with the exception of the vascular fraction which was fixed at 0.25 for the dog study and 0.40 for the human study. In general, fixing and constraining the other parameters in the two-compartment model reduced the interquartile range for k_{21} by at least one-third. Variability of the one-compartment model parameters was not significantly reduced.

Goodness-of-Fit Model Comparisons

The mean description lengths (*DL*) for the fits of each model to the noisy simulated data are shown in Figure 7, with separate plots for the 5%, 10% and 20% noise simulations. With 5% or 10% noise, the two-compartment model has a smaller description length than either the one-compartment model or the three-compartment model which generated the data. The one-compartment model description length increases with flow and the increase is greater at the lower noise levels. With 20% noise the one-compartment model gives fits which are more comparable to the other two models, having a description length which is somewhat less than the others at low flow and somewhat greater at high flow.

Description lengths computed for fits to the sample dog and human PET study data fell in the range 120 - 130, similar to the 20% noise case in the simulations. For the two compartment model, the mean high flow (stress) values of *DL* were 126 and 128, respectively, in the dog and human studies. The mean low flow (rest) values were 129 in both dog and human studies. Simulation data predicted higher values of DL for high flow studies with the same noise level, but noise levels were lower in the stress data (see Methods section for discussion). The description length criterion does not significantly differentiate between the one- and two-compartment models. This outcome is predicted by the simulations at low flow, but at high flow with less than 20% noise the simulations predict a measurably better fit by the two-compartment model.

Discussion

Taking a three-compartment physiological model as a reference point, we have compared two reduced-order models and have examined some of the consequences of the model misspecifi-

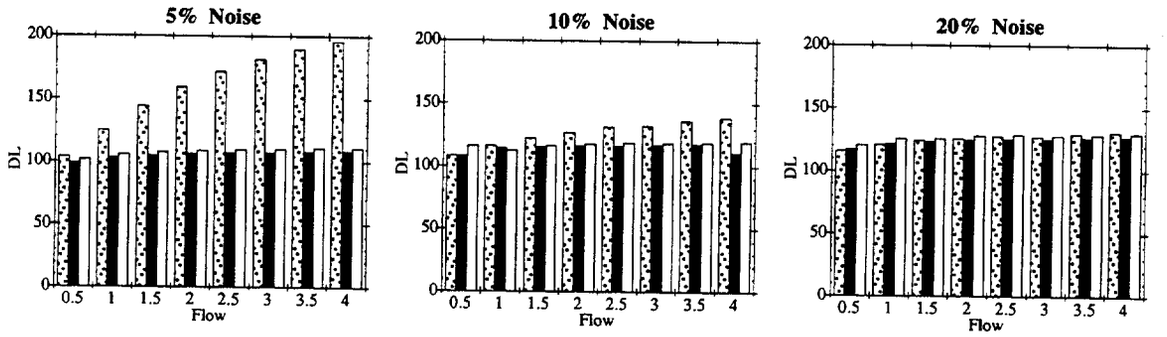

Figure 7: Description lengths for model fits to simulated data for 5%, 10%, and 20% noise levels. The mean description lengths computed from fits of the three-compartment model as well as both reduced-order models are shown with eight sets of bars corresponding to the eight flow rates. The speckled bars represent the 1-compartment model, the dark solid bars represent the 2-compartment model, and the white bars represent the true three-compartment model.

cation in both cases. Specific model misspecification artifacts included parameter bias and systematic parameter variation where none was expected. In the two-compartment model both flow and volume are underestimated. In the one-compartment model, all three model parameters increased with flow.

Monte Carlo simulations provided insight into the additional bias and variation induced by errors in the PET measurement data. Two parameters (k_{12} and k_{32}) of the two-compartment model were particularly sensitive to the noise. Variability of the k_{21} estimates was reduced when other parameter values were fixed or constrained. When the two reduced-order models were fit to actual PET data sets, the parameter estimates were generally consistent with the simulation results. The two-compartment model parameter estimates were more variable than the estimates based on simulated data. This difference was expected due to the smaller sample size, but the magnitude of the difference may reflect the presence of errors and variation not accounted for in the model simulations. The variability of k_{21} estimates for the PET data was reduced by fixing the other parameters, even though the values chosen were based on the simulated conditions and not the true parameter values which of course are not known.

The description length goodness-of-fit criterion computed for all three models showed that the two-compartment model fit the simulated data very well at noise levels from 5% to 20% and that the one-compartment models fit relatively poorly, especially at high flow values, except at the 20% noise level. Fits to the actual PET data sets differed in that the description length was about the same or slightly lower for both reduced-order models at the higher flow rate. Also, the one-compartment model gave a fit that was as good or better than the two-compartment model, even at high flow.

Conclusions

The noise-free and Monte Carlo simulations taken together help us to assess the ability of both models to estimate underlying physiological parameters and to differentiate between relevant clinical states. The two-compartment model provides, in theory, a good representation of the three-compartment reference model and the possibility of obtaining estimates of permeability surface products, volumes, and flow with only small misspecification error. Measurement error, however, erodes the parameter estimate accuracy so that it is difficult to use the model for this purpose. The one-compartment model is substantially better at differentiating flow in the lower range and is also better in the range of clinical interest. The two-compartment model can differentiate flow only if *a priori* values are used for non-flow parameters.

The use of simplified models for PET kinetic analysis is a standard practice, necessitated by measurement limitations and variability. This study has helped us to understand the consequences of this practice in a particular example.

Acknowledgments

Sophanie Lim, Bryan Reutter and Gregory Klein contributed technical and programming support for this project. Several of the figures and some preliminary results for this work appeared in a conference report [22]. Thoughtful suggestions from two reviewers helped to improve the exposition. The work was supported in part by the National Heart, Lung and Blood Institute of the U.S. Department of Health and Human Services under Grants No. HL47675, HL25840 and HL07367, and in part by the Director, Office of Energy Research, Office of Health and Environmental Research, Medical Applications and Biophysical Research Division of the U.S. Department of Energy under Contract No. DE-AC03-76SF00098.

References

[1] Budinger TF, Huesman RH, Knittel B, Friedland R, and Derenzo SE. Physiological modeling of dynamic measurements of metabolism using positron emission tomography. In Greitz T and Ingvar D, editors, *The Metabolism of the Human Brain Studied with Positron Emission Tomography*, pages 165–183. Raven Press, New York, 1985.

[2] Tancredi RG, Yipintsoi T, and Bassingthwaighte JB. Capillary and cell wall permeability to potassium in isolated dog hearts. *Am J Physiol* 1975; 229:537-544.

[3] Goresky CA, Ziegler WH, and Bach GG. Capillary exchange modeling: Barrier-limited and flow-limited distribution. *Circ Res* 1970; 27:739-764.

[4] Bassingthwaighte JB, Chan IS, and Wang CY. Computationally efficient algorithms for capillary convection-permeation-diffusion models for blood-tissue exchange. *Ann Biomed Eng* 1992; 20:687-725.

[5] Budinger TF, Derenzo SE, Huesman RH, Cahoon JL, Vuletich T. Dynamic positron emission tomograph with 2.5 mm resolution. in Hayaishi O and K Torizuka, ed., *Biomedical Imaging* pages 17–33, Academic Press, Tokyo, 1986.

[6] Derenzo SE, Huesman RH, Cahoon JL, Geyer AB, Moses WW, Uber DC, Vuletich T, Budinger TF. A positron tomograph with 600 BGO crystals and 2.6 mm resolution. *IEEE Trans Nucl Sci* 1988; NS-35(1):659–664.

[7] Hoffman EJ, Huang SC, Phelps ME, Kuhl DE. Quantitation in positron emission computed tomography: 4. Effect of accidental coincidences. *J Comput Assist Tomogr* 1981; 5(3):391–400.

[8] Hoffman EJ, Huang SC, Plummer D, Phelps ME. Quantitation in positron emission computed tomography: 6. effect of nonuniform resolution. *J Comp Assist Tomogr* 1982; 6(5):987–999.

[9] Mazoyer BM, Huesman RH, Budinger TF, Knittel BL. Dynamic PET data analysis. *J Comput Assist Tomogr* 1986; 10(4):645–653.

[10] Jagust WJ, Budinger TF, Huesman RH, Friedland RP, Mazoyer BM, Knittel BL. Methodologic factors affecting PET measurements of cerebral glucose metabolism. *J Nucl Med* 1986; 27(8):1358–1361.

[11] Huang SC, Hoffman EJ, Phelps ME, Kuhl DE. Quantitation in positron emission computed tomography: 3. Effect of sampling. *J Comput Assist Tomogr* 1980; 4(6):819–826.

[12] Herrero P, Markham J, Shelton ME, Bergmann SR. Implementation and evaluation of a two-compartment model for quantification of myocardial perfusion with rubidium-82 and positron emission tomography. *Circ Res* 1992; 70:496–507.

[13] Huang SC, Williams BA, Krivokapich J, Araujo L, Phelps ME, and Schelbert HR. Rabbit myocardial ^{82}Rb kinetics and a compartmental model for blood flow estimation. *Am J Physiol* 1989; 256:H1156–H1164.

[14] Coxson PG, Brennan KM, Huesman RH, Lim S, and Budinger TF. Variability and reproducibility of rubidium-82 kinetic parameters in the myocardium of the anesthetized canine. *J Nucl Med* 1995; 36:287–296.

[15] Deussen A, and Bassingthwaighte JB. Modeling [^{15}O]-oxygen tracer data for estimating oxygen consumption. *Am. J. Physiol.*, 270(Heart Circ. Physiol. 39):H1115-1130, 1996.

[16] Bassingthwaighte JB, Yipintsoi T, and Harvey RB. Microvasculature of the dog left ventricular myocardium. *Microvasc Res* 1974; 7:229-249.

[17] Conn HL Jr., Robertson JS. Kinetics of potassium transfer in the left ventricle of the intact dog. *Am J Physiol* 1954; 181:319-324.

[18] Sheehan RM, and Renkin EM. Capillary, interstitial and cell membrane barriers to blood-tissue transport of potassium and rubidium in mammalian skeletal muscle. *Circ Res* 1972; 30:588-607.

[19] Coxson PG, Salmeron EM, Huesman RH, and Mazoyer BM. Simulation of compartmental models for kinetic data from a positron emission tomograph. *Comput Methods Programs Biomed* 1992; 37:205–214.

[20] Huesman RH, Klein GJ, Reutter BW, Coxson PG, Botvinick EH, and Budinger TF. Strategies for extraction of quantitative data from volumetric dynamic cardiac PET data. *Cardiology* 1996 (in press).

[21] Rissanen, J. *Stochastic complexity in statistical inquiry.* Teaneck, N.J.: World Scientific, Series in computer science; vol. 15, 1989.

[22] Coxson PG, Huesman RH, Lim S, Klein GJ, Reutter BW, and Budinger TF. Comparison of kinetic models for data from a positron emission tomograph. In: E. Hoffman eds *Medical Imaging 1995: Physiology and Function from Multidimensional Images.* Bellingham, WA: SPIE, 1995; 2433:224–234.